$$C_p = w^2 \, \alpha_p{}^2 \, T \, M / (\gamma - 1)$$
$$= w^2 \, \alpha_p{}^2 \, T \, M / (\varkappa_T \, w^2 \, M / V - 1) \quad (8)$$

where M is the molar mass. The vaues for α_p, $\varkappa_T$, and V were calculated from Equation (3). The estimated error of the heat capacities at normal pressure calculated from Eqs. (6) to (8) is about 15%. In spite of such a large uncertainty a decrease of $C_p(P_0, T)$ with increasing temperature can be established from Fig. 7, although it may not be as pronounced as shown in the figure. A negative temperature dependence of the molar heat capacity, although somewhat exceptional, was also evaluated from Monte Carlo calculations for molten KCl[7] (see also Section 4 and Table 3) and from molecular dynamics calculations for molten NaCl[37]. It was also found experimentally for fused $NaNO_3$ and KNO_3[36] as well as for some other liquids, e. g. water[38] and mercury[39]. For higher pressures the sign of the temperature dependence of the heat

Fig. 9. Molar heat capacity at constant volume versus pressure. $- \cdot - \cdot -$ extrapolation beyond stability range of liquid phase.

capacity remains the same, but it appears from Fig. 7 that the molar heat capacity probably passes a minimum at temperatures above 1100 °C.

The temperature independent heat capacity values at 1 bar reported in the literature[30, 32–34] ranging from 67.0 to 74.2 $J \, mol^{-1} K^{-1}$ correspond to some intermediate values in the temperature interval covered by the $P V T$ experiments.

The molar heat capacity C_p also decreases slightly with increasing pressure (Figure 8).
Figure 9 shows the molar heat capacity at constant volume C_V calculated from

$$C_p - C_V = \alpha_p{}^2 \, T \cdot V / \varkappa_T \quad (9)$$

as a function of pressure. Since the uncertainties in C_V are considerable, the change in sign of its pressure dependence may or may not be real. C_V also decreases with increasing temperature for constant density as well as for constant pressure.
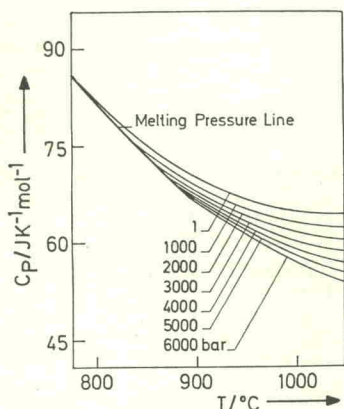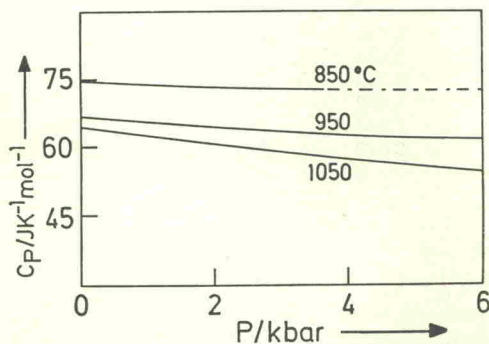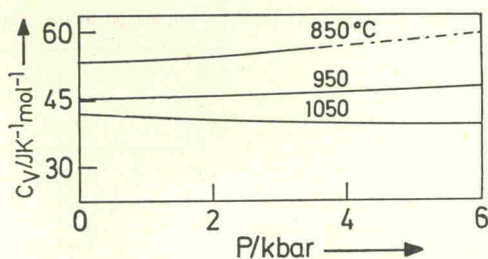

Fig. 7. Molar heat capacity at constant pressure versus temperature.

Fig. 8. Molar heat capacity at constant pressure versus pressure. $- \cdot - \cdot -$ extrapolation beyond stability range of liquid phase.

4. Comparison with Computer Simulations

The first and most extensive computer simulation experiments for molten salts have been performed on potassium chloride. Woodcock and Singer[7] employed the Monte Carlo method to calculate the macroscopic properties of KCl using the Huggins-Mayer pair potential with constants determined by Fumi and Tosi[40] from the properties of the crystal at 298 K. Five of their calculated $P V T$ points fall into the density range of the experiments. They are compiled in Table 2. The maximum difference between experimental and calculated densities amounts to 2%, corresponding to a pressure difference of 850 bar. MC computations by Larsen, Førland, and Singer[41] gave $P V T$ data with density values which are low by about 4%. Preliminary density values obtained by Lewis[42] from molecular dynamics cal-

Table 2. Comparison of computer simulation results with experimental data.

Reference	T_{cal} [°C]	ϱ_{cal} [g cm⁻³]	P_{cal} [bar]	ϱ_{exp} (T_{cal}, P_{cal}) [g cm⁻³]	$100(\varrho_{cal}-\varrho_{exp})/\varrho_{exp}$ [%]	P_{exp} (T_{cal}, ϱ_{cal}) [bar]	$P_{cal}-P_{exp}$ [bar]
Woodcock	772	1.608	2820	1.635	−1.7	1967	853
and	772	1.528	670	1.558	−2.0	29	641
Singer [7]	1033	1.528	3710	1.560	−2.0	2856	854
	1033	1.455	1440	1.465	−0.7	1260	180
	1033	1.389	(−30)	1.372	+1.3	195	−225
Larsen	810	1.439	1	1.504	−4.3		
et al. [41]	810	1.491	810	1.544	−3.4		

Table 3. Comparison of computer simulation results [7] with experimental data.

T [°C] cal	P [bar] cal	$10^4 \alpha_p$ [K⁻¹] cal	exp	$10^6 \varkappa_T$ [bar⁻¹] cal	exp	β_V [bar K⁻¹] cal	exp	P_i [kbar] cal	exp	C_p [J K⁻¹ m⁻¹] cal	exp
772	2820	2.33	2.56	19.2	18.2	12.1	14.1	12.6	8.6	60.9	84.2
772	670	3.04	3.41	30.6	24.0	9.92	12.1	10.4	8.6	67.3	85.7
1033	3710	0.35	2.52	4.04	23.0	8.66	11.1	11.3	7.7	45.3	58.1
1033	1440	2.19	3.24	30.2	34.3	7.24	9.5	9.45	8.2	56.0	61.1
1033	(−30)	3.37	4.24	52.5	57.0	6.42	7.1	8.38	7.6	61.5	64.1

Table 4. Comparison of estimated (Eq. (11)) with measured densities.

Salt	$10^6 \varkappa_T$ (1 bar, T) [bar⁻¹]	B Eq. (10) [bar]	T [°C]	P [bar]	ϱ_{est} [g cm⁻³]	ϱ_{exp} [g cm⁻³]	$100(\varrho_{est}-\varrho_{exp})/\varrho_{exp}$ [%]
KCl	38.4 [28]	2358	800	1000	1.566	1.558 [6]	0.5
	45.7	1987	900	1000	1.514	1.508	0.4
			900	5000	1.661	1.647	0.8
	54.7	1667	1000	1000	1.462	1.458	0.3
			1000	5000	1.618	1.613	0.3
KNO₃	23.4 [28]	3769	400	1000	1.869	1.864 [2]	0.3
			400	5000	1.992	1.978 [4]	0.7
			400	10000	2.095	2.091 [4]	0.2
	29.4	3008	500	1000	1.804	1.796 [2]	0.4
			500	5000	1.941	1.938 [4]	0.2
			500	10000	2.051	2.047 [4]	0.2
NaNO₃	21.6 [28]	4080	400	1000	1.894	1.886 [2]	0.4
			400	5000	2.014	2.022 [4]	−0.4
			400	10000	2.115	2.157 [4]	−1.9
	26.8	3296	500	1000	1.832	1.818 [2]	0.8
			500	5000	1.964	1.966 [4]	−0.1
			500	10000	2.072	2.106 [4]	−1.6

culations with the same pair potential as has been used by Woodcock and Singer fall about 7% below the experimental results. Recent MC calculations on molten potassium chloride using the Pauling potential [43] or including ionic polarization effects [44] yielded even less satisfactory results. The calculated density values at the melting temperature at 1 bar are low by 15.8 and 12.8%, respectively. MC computations on other molten salts by Lewis, Singer, and Woodcock (see [43]) also using the Huggins-Mayer potential led in most cases to larger discrepancies with experimental data than for KCl.